Temporal Correlation-Based Measurements of Signal Lag

Arpit Sourav Mohapatra,
College of Engineering Bhubaneswar

***Abstract*—A flat-panel dynamic radiography detector can be used to obtain x-ray image sequences during fluoroscopic imaging. The sequential acquisition of pictures results in lag signals and lag artifacts due to charge trapping at photodiodes. It is crucial to precisely measure the lag signal in order to construct low-lag detectors. To get a real noise power spectrum under the IEC62220-1-3 standard, a lag correction factor (LCF) is determined and steady-state pictures are used to calculate a temporal power spectral density (PSD). However, a variety of noise signals can quickly skew the PSD curve and result in inaccurate LCF values. In this letter, we present a linear lag model-based measurement technique for LCF based on correlation coefficients from steady-state pictures. This approach may be a generalized form of an approach with a resistance to different kinds of sounds feature, which is based on the first-order regression model. As a result, the suggested algorithm may serve as a substitute for the PSD method in the standard.**

***Index Terms*—Flat-panel dynamic radiography detector, fluoroscopy imaging, lag correction factor, power spectral density.**

I. Introduction

INHERENT noise properties of radiography detectors from photon and electric noise can be investigated by measuring the *noise power spectrum* (NPS) using x-ray images acquired under specified irradiation conditions with uniform intensity [1]. In fluoroscopy imaging, flat-panel (FP) dynamic detectors can acquire x-ray image sequences with frame rates up to 300 frames per second (fps). However, the sequentially acquired images have *lag signals* from previous frames. For indirect detectors, trapping charges in photodiodes, which are controlled by the amorphous Si or In-Ga-Zn-O (IGZO) thin film transistor (TFT) panel, and incomplete readouts are major causes of the lag signals.

In measuring the NPS from an image sequence acquired from a dynamic detector, the lag signal lowers the NPS curve. Hence, in order to observe the true NPS performance of a dynamic detector, developing a measurement technique, which is independent of the lag signal, is required. Conventional approaches for correcting the measured NPS from the lag signal are based on using the *lag correction factor* (LCF). Granfors and Aufrichtig [2] calculated LCF using decaying transient image means after the x-ray tube turns off based on a linear lag model. Here, a synchronized pulse x-ray source for the pulsed fluoroscopy mode should be employed to accurately measure the means.

The standard of IEC62220-1-3 [3] recommends using a constant potential generator for the continuous fluoroscopy mode to evaluate the detector lag performance. Busse *et al.* [4] used a temporal power spectral density (PSD) method to measure LCF using stead-state images and thus is employed in the standard [5]. However, due to the nonuniform temporal gain, which occurs from the transient responses of the lag and x-ray tube, and pixel offset, which occurs from nonuniform gate drive and readout circuits, accurately measuring PSD for LCF is difficult especially at low frequencies [6]–[9].

Underlying a first-order autoregression (AR(1)) model, we can measure a LCF from the decaying transient image means or the correlation coefficient from the steady-state images [10], [11]. In this letter, we propose a measurement algorithm for LCF using the correlation coefficients from steady-state images based on a linear lag model. This method can be a generalized version of the AR(1) method and has a characteristic that is resistant to noise compared to the PSD method. Hence, for IEC62220-1-3, the proposed algorithm can be an alternative approach to the PSD method.

This letter is organized in the following way. In Section II, a linear model is introduced to describe the lag signals. The measurement of NPS with the lag signal is then observed. In Section III, the proposed measurement algorithm for LCF is introduced and a practical consideration for acquired images is introduced. Experimental results using x-ray images acquired from dynamic detectors are shown in Section IV. The letter is concluded in the last section.

II. Noise Power Spectrum and Its Lag Correction

In this section, an image sequence model for dynamic radiography detectors is formulated with NPS measurements and a linear lag model is introduced with a lag correction scheme.

A. Linear Lag Model and the Lag Correction Factor

For a sequence of uniformly exposed images, we consider a weakly stationary sequence $f_n[\boldsymbol{u}]$ with the mean of $\mu := E\{f_n\}$ and variance of $\sigma^2 := \mathrm{Var}\{f_n\}$, for the pixel position $\boldsymbol{u}$ of the nth image frame, where $\boldsymbol{u} \in \mathsf{U}^2$ and $\mathsf{U} := \{0, \ldots, U-1\}$. Let I_f denote the mean of the periodogram of f as

$$I_f[\boldsymbol{v}] := E\left\{ \left| \frac{1}{U^2} \sum_{\boldsymbol{u} \in \mathsf{U}^2} (f_n[\boldsymbol{u}] - \mu) W^{\boldsymbol{u}^{\mathrm{T}}\boldsymbol{v}} \right|^2 \right\}, \quad (1)$$

for $\boldsymbol{v} \in \mathbb{U}^2$, where $W_U := e^{-2\pi j/U}$. Let NPS_f denote the NPS of f for the nth frame. We then have an asymptotic relationship: $I_f \to NPS_f$, as $U \to \infty$. For practical measurements using the acquired f_n, we can obtain I_f from a smoothed periodogram of a sample mean of the periodogram based on the Bartlett-Welch method [12], [13].

We now introduce the conventional lag model based on a linear, time-invariant system [2], [4], [5], [14], [15]. Let us consider an independent and identically distributed random sequence g_n along the frame with an impulse response h_A. Here, we suppose that h_A is a causal system, i.e., $h_A = 0$, for $A < 0$, and $E\{g_n\} = \mu$, $\forall n$. The linear lag model can then be given as

$$f_n[\boldsymbol{u}] = \sum_{A=0}^{\infty} g_{n-A}[\boldsymbol{u}] \cdot h_A, \tag{2}$$

where $\sum_{A=0}^{L-1} h_A = 1$ and $L - 1$ is the filter dimension. From (2), I_f satisfies $I_f[\boldsymbol{v}] = r \cdot I_g[\boldsymbol{v}]$, where I_g is the mean of the periodograms of g and converges to the NPS of g, which is denoted as NPS_g. Here, r is the LCF for the linear model of (2) and is defined as [2], [4]

$$r := \sum_{A=0}^{\infty} h_A^2. \tag{3}$$

In order to asymptotically recover NPS_g, we can use an estimate of r to correct the measured NPS_f as $NPS_g[\boldsymbol{v}] \approx NPS_f[\boldsymbol{v}]/r \approx I_f[\boldsymbol{v}]/r$. Here, NPS_g is the NPS of the given radiography detector under the assumption that there is no lag. The standard of ICE62220-1-3 mentions that a noise property of a dynamic detector is characterized by measuring NPS_g by removing the influence from the lags [3]. Because r satisfies $0 < r \leq 1$, the measured NPS of f is usually less than the NPS without lags. Hence, in order to measure the true detector NPS, which is independent of lags, the measured NPS with lags should be corrected.

B. Lag Correction Factor From the Temporal Periodograms

Let J_f denote the mean of the periodogram of f along the frame n. J_f is then defined as

$$J_f[k] := E\left\{ \frac{1}{N} \left| \sum_{n=0}^{N-1} (f_n[\boldsymbol{u}] - \mu) W_N^{nk} \right|^2 \right\}, \tag{4}$$

which is an asymptotically unbiased estimate of the temporal PSD of f as N increases. We then have $J_f[k] = |H_k|^2 \cdot J_g[k]$, where H_k is the discrete Fourier transform of h_A and J_g is the periodogram mean of g in a similar manner of (4) [16, p. 67]. From the independent assumption on g_n along n, J_g is constant. Because $H_0 = 1$, we then have $J_f[k] = |H_k|^2 \cdot J_f[0]$, where $J_f[0]$ is an estimate of the PSD of f at zero frequency [7], [17]. Therefore, from Parseval's theorem, the LCF of (3) satisfies $r = N^{-1} \sum_{k=0}^{N-1} |H_k|^2$ and thus

$$r = \frac{\frac{1}{N} \sum_{k=0}^{N-1} J_f[k]}{J_f[0]} \tag{5}$$

holds [4], [5]. Hence, in order to estimate the LCF of r, we can use the relationship (5). We call this estimate method from the temporal PSD or periodograms the PSD method.

III. Lag Correction Based on Temporal Correlations

In this section, we propose a novel LCF measurement approach, which uses the correlation coefficients from stead-state images.

For a given n, define an image difference $\Delta f_n[\boldsymbol{u}]$ as $\Delta f_n[\boldsymbol{u}] := (f_n[\boldsymbol{u}] - f_0[\boldsymbol{u}])/\sqrt{2}$, for $n = 0, \ldots, L - 1$. From Appendix, I_g, the periodogram mean of g, satisfies

$$I_g[\boldsymbol{v}] = (2L - 1) I_f[\boldsymbol{v}] - 2 \sum_{A=0}^{L-1} I_{\Delta f_1}[\boldsymbol{v}] \tag{6}$$

and thus, the detector NPS can be measured from $NPS_g[\boldsymbol{v}] \approx I_g[\boldsymbol{v}]$ without estimating LCF.

Using the image differences Δf_n, we can also estimate LCF as follows. From the periodogram relationship of (6), we can obtain a relationship between the variances of f_n and g_n as

$$\mathrm{Var}\{g_0\} = 2 \sum_{A=0}^{L-1} \mathrm{Cov}\{f_0, f_A\} - \mathrm{Var}\{f_0\}. \tag{7}$$

Let ρ_A denote the Pearson correlation coefficient of f and be defined as $\rho_A := \mathrm{Cov}\{f_0, f_A\}/\mathrm{Var}\{f_0\}$, for $A = 0, \ldots, L - 1$. Hence, from $\mathrm{Var}\{f_0\} = r\,\mathrm{Var}\{g_0\}$ and (7), the LCF of (3) can be given as

$$r = \frac{1}{2 \sum_{A=0}^{L-1} \rho_A - 1}, \tag{8}$$

which is employed in the proposed correlation algorithm.

For the lag signals, if we consider a AR(1) model as in [10], [11], then a different lag model can be given as

$$f_n[\boldsymbol{u}] = a f_{n-1}[\boldsymbol{u}] + (1 - a) g_n[\boldsymbol{u}]. \tag{9}$$

For the model of (9), we have $I_f[\boldsymbol{v}] = I_g[\boldsymbol{v}] \cdot (1 - a)/(1 + a)$. Here, the corresponding LCF is given as $(1 - a)/(1 + a)$. Assume that the correlation coefficients ρ_A satisfies $\rho_A = a^A$, for $A = 0, 1, \ldots$. Then, the LCF of (8) satisfies $\lim_{L \to \infty} r = (1 - a)/(1 + a)$, which is equal to that of the AR(1) model. Hence, if a in the AR(1) model is measured from the correlation coefficient, then the LCF in (8) can be a generalized version of the AR(1) case if $L \to \infty$.

We now introduce the correlation algorithm based on the estimate of (8) for a noisy environment. For practical dynamic detectors, the acquired images contain the electrical and fixed pattern noise as well as the photon noise. Hence, for the exposed images, we consider an image formation model as

$$q_n[\boldsymbol{u}] := f_n[\boldsymbol{u}] + \xi_n[\boldsymbol{u}] + \zeta[\boldsymbol{u}], \tag{10}$$

where ξ_n implies the electrical noise and ζ implies a fixed pattern noise from the exposure. We assume that the three terms in (10) are mutually independent. The variance of q_n is then given as

$$\mathrm{Var}\{q_n\} = \mathrm{Var}\{f_n\} + \mathrm{Var}\{\xi_n\} + \mathrm{Var}\{\zeta\}, \tag{11}$$

and the covariance between q_0 and q_n is given as

$$\mathrm{Cov}\{q_0, q_n\} = \mathrm{Cov}\{f_0, f_n\} + \mathrm{Cov}\{\xi_0, \xi_n\} + \mathrm{Var}\{\zeta\}. \tag{12}$$

Here, we assume that $\mathrm{Cov}\{q_0, q_n\} = \mathrm{Var}\{\zeta\}$ for $n \geq L$. For the dark images, which are acquired without the exposures, the variance of (11) becomes $\mathrm{Var}\{\xi_n\}$ and the covariance of (12) becomes $\mathrm{Cov}\{\xi_0, \xi_n\}$. Hence, we can obtain $\sigma^2 = \mathrm{Var}\{f_n\}$ and

TABLE I
FLAT-PANEL DYNAMIC DETECTORS FOR THE EXPERIMENTS

Detector		Description	Binning
A	DRTECH EXPD	a-IGZO TFT/photodiode/CsI 1,628× 1,628pixels, 98μm/pixel	1× 1
B	TRIXELL Pixium RF4343	a-Si TFT/photodiode/CsI 900× 900pixels, 148μm/pixel	3× 3

Cov$\{f_0, f_n\}$ from (11) and (12). We now summarize a measurement algorithm for LCF based on the temporal correlations as follows.

Temporal Correlation Algorithm:

1) Calculate Var$\{q_n\}$ and Cov $\{q_0, q_n\}$ using uniformly exposed images, for $n = 0, \ldots, L$.
2) Obtain the variance of ζ from Var $\{\zeta\}$ = Cov $\{q_0, q_L\}$
3) From the dark images, obtain Var$\{\xi_n\}$ and Cov $\{\xi_0, \xi_n\}$ for $n = 0, \ldots, L - 1$.
4) From (11) and (12), calculate Var$\{f_n\}$ and Cov $\{f_0, f_n\}$ respectively, to obtain LCF from (8).

In order to obtain an accurate Var$\{\zeta\}$, we can use many estimates of Cov$\{q_0, q_n\}$, for $n \geq L$, instead of a single Cov$\{q_0, q_L\}$.

IV. EXPERIMENTAL RESULTS

In this section, experimental results for the LCF measurements for flat-panel dynamic detectors are introduced. The detectors, which were employed in the experiment, are summarized in Table I. The x-ray image sequences were acquired under the RQA 5 condition of IEC62220-1-3 [3] at a continuous fluoroscopy mode with the frame rates of 10 and 20fps. Here, a constant potential high-voltage generator was used for the x-ray source [3].

In acquiring image sequences, the image gain of each image frame is not uniform. Hence, the nonuniform temporal gain should be corrected to accurately estimate LCF when the PSD method is used [4]. In order to describe the nonuniform gain, we can introduce a weakly stationary random sequence γ_n with mean 1 and variance σ_γ^2, and modify the image sequence q_n as $\gamma_n q_n$. Here, the gain γ_n is independent of the pixels of $\boldsymbol{u}$. For a given n, a conditional estimate of $\gamma_n \mu$ over the pixels of $\boldsymbol{u}$ can be obtained. Furthermore, we can empirically obtain an estimate of μ over n and $\boldsymbol{u}$. Hence, by multiplying the ratio $1/\gamma_n$ to the nth frame, we can correct the nonuniform gains.

Instead of the multiplication, we can use an image difference if $1 \gg \sigma_\gamma^2$, as described in [18, Image Difference Algorithm]. Note that this difference approach can alleviate nonuniform offsets as well as gains [19], [20]. For the nth image frame with $U \times U$ pixels, calculate the image differences between the upper and lower pixels as

$$\frac{1}{\sqrt{2}}\left[\gamma_n q_n[\boldsymbol{u}] - \gamma_n q_n[\boldsymbol{u} + (0, U/2 - 1)]\right], \qquad (13)$$

for $\boldsymbol{u} \in [0, \ldots, U - 1] \times [0, \ldots, U/2 - 1]$. Using the image difference of (13), we can calculate the temporal periodogram of (4) and then LCF from (5). We call this difference scheme of (13) the *U-L correction*. Here, we assume that pixels, which are separated by $U/2$, are mutually independent as the α-mixing condition [21].

In Fig. 1, an example of the temporal PSD curves of J_f are illustrated to show the distorted spectrum from the nonuniform

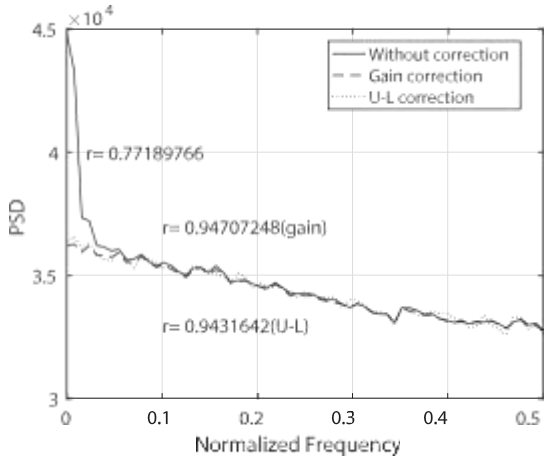

Fig. 1. Comparison of the PSD curves and LCF estimates from the PSD method of IEC62220-1-3 [3]. The image sequence was acquired from Detector A with an incident exposure of 2,255nGy, frame rate of 10 fps, and a periodogram size of $N = 128$. The PSD curves of the dark images were subtracted.

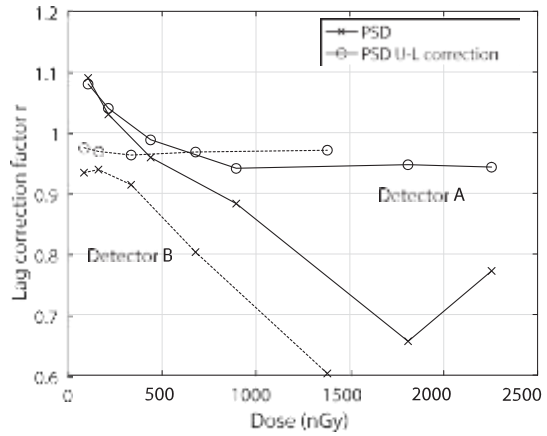

Fig. 2. LCF estimates from the PSD method and the temporal gain correction with respect to the incident dose. The frame rate and periodogram size were 10fps and $N = 128$, respectively. Applying the U-L correction can reduce estimate errors.

temporal gain. If we do not conduct any gain correction, then the spectrum at low frequencies is inflated and thus the LCF estimate is usually lower than the true LCF because the PSD at zero frequency $J_f[0]$ is a reference in calculating LCF from (8) [7], [17]. Applying a gain or the U-L correction can remove the inflated spectrum and thus can yield accurate LCF values. LCF estimates from the PSD method for different incident doses are illustrated in Fig. 2. When we did not apply any gain correction as "PSD" in Fig. 2, the estimate accuracies were bad with respect to the dose. Applying the U-L correction to alleviate the nonuniform gain problem yielded relatively good estimate accuracy as "PSD U-L correction" in Fig. 2.

Estimates of LCF from the proposed temporal correlation algorithm are illustrated in Fig. 3. We can observe that the LCF estimates are independent of the nonuniform gains as "Corr." and "Corr. U-L correction." Hence, we can obtain reliable LCF values from the proposed correlation algorithm without carefully considering various noises. In Fig. 4, the LCF estimate from the proposed correlation algorithm is compared with that of the PSD method for the U-L corrected images. We can observe that both methods yield similar LCF values. As shown in Figs. 2–4, the

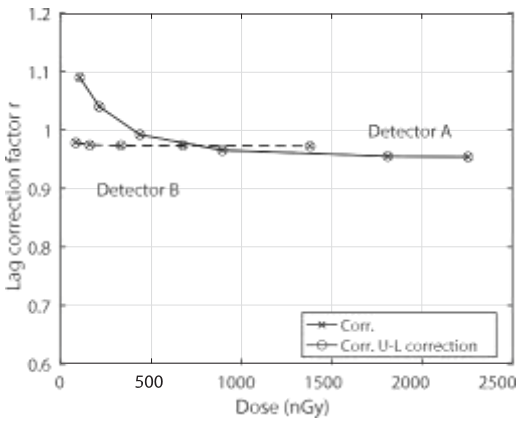

Fig. 3. LCF estimates from the proposed correlation method. The frame rate was 10fps and 128 image frames were used to estimate ρ_A for $L = 4$.

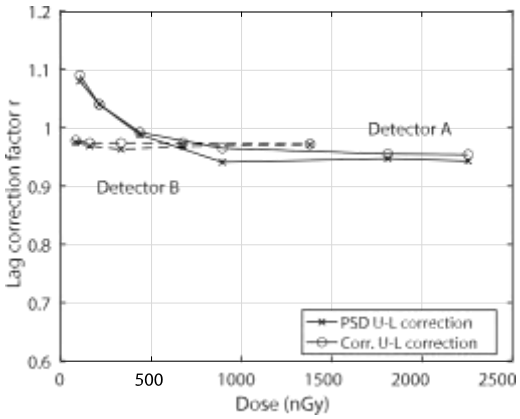

Fig. 4. Comparison of the LCF estimates from the proposed correlation and conventional PSD methods of Figs. 2 and 3. The U-L correction was conducted to correct the nonuniform temporal gains.

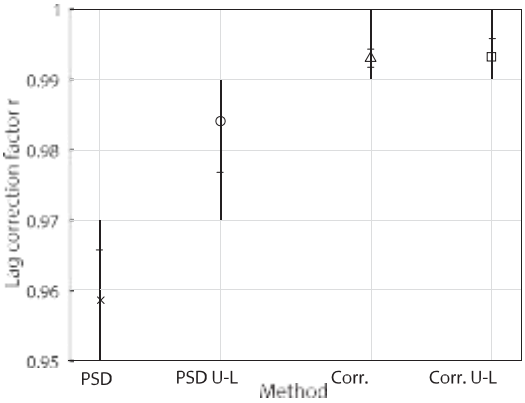

Fig. 5. Comparison of the means and standard deviations of the estimates for Detector A (20 fps) at the incident dose of 447nGy per frame. Each result was calculated by conducting measurements 10 times.

estimates of $r > 1$ especially at low doses shows a phenomenon occurred from second moment-based approaches, such as the PSD and proposed correlation methods. In fact, the LCF values are slightly reduced at low doses in contrast to increasing incorrect estimates [4], [22], [23]. In Fig. 5, the means and standard deviations of the LCF estimates are illustrated at 447nGy. We can observe that the estimate precision of the proposed correlation algorithm is much better than the PSD case and is getting better as the dose increases.

V. Conclusion

This letter suggested an LCF measuring algorithm based on steady-state image frames' temporal correlation coefficients. When compared to the traditional PSD approach of IEC62220-1-3, the suggested correlation algorithm demonstrated reduced sensitivity to different noises.

Appendix
I_g: Periodogram Mean of g

From the lag model of (2), the image difference Δf_A can be rewritten as

$$\Delta f_A = \frac{1}{\sqrt{2}} \sum_{k=0}^{L+A-1} (h_k - h_{k-A}) \cdot g_{A-k}, \qquad \text{(A1)}$$

for $l = 0, \ldots, L - 1$. The mean of the periodogram of Δf_A can then be expanded as

$$I_{\Delta f_A}[v] = \frac{1}{2} \sum_{k=0}^{L+A-1} (h_k - h_{k-A})^2 I_g[v]$$

$$= r - \sum_{k=A}^{L-1} h_k h_{k-A} \; I_g[v]. \qquad \text{(A2)}$$

From (A2), we can obtain a relationship as

$$I_f[v] - I_{\Delta f_A}[v] = \sum_{k=A}^{L-1} h_k h_{k-A} \; I_g[v]. \qquad \text{(A3)}$$

The mean of the periodogram of g can be expanded as

$$I_g[v] = \sum_{A=0}^{L-1} h_A^2 \; I_g[v]$$

$$= r + 2 \sum_{A=0}^{L-1} \sum_{k=A}^{L-1} h_k h_{k-A} \; I_g[v]$$

$$= 2 \sum_{A=0}^{L-1} \sum_{k=A}^{L-1} h_k h_{k-A} - r \; I_g[v]. \qquad \text{(A4)}$$

From (A3) and (A4), we can obtain the relationship of (6).

References

[1] G. M. Jenkins and D. G. Watts, *Spectral Analysis and Its Applications*. San Francisco, CA, USA: Holden-Day, 1969.

[2] P. R. Granfors and R. Aufrichtig, "DQE(f) of an amorphous-silicon flat-panel X-ray detector: Detector parameter influences and measurement methodoloty," in *Proc. SPIE, Med. Imag.: Phys. Med. Imag.*, vol. 3977, 2000, pp. 2–13.

[3] International Electrotechnical Commission, *Medical Electrical Equipment Characteristics of Digital X-ray Imaging Devices-Part1-3: Determination of the Detective Quantum Efficiency Detectors used in Dynamic Imaging*. Geneva, Switzerland: IEC 62220-1-3, 2007.

[4] F. Busse *et al.*, "Methodology to measure fundamental performance parameters of X-ray detectors," in *Proc. SPIE, Med. Imag.: Phys. Med. Imag.*, vol. 4320, 2001, pp. 287–298.

[5] B. Menser, R. J. M. Bastiaens, A. Nascetti, M. Overdick, and M. Simon, "Linear system models for lag in flat dynamic X-ray detectors," in *Proc. SPIE, Med. Imag.: Phys. Med. Imag.*, vol. 5745, 2005, pp. 430–441.

[6] D. S. Kim, "High precision noise power spectrum measurements in digital radiography imaging," *Med. Phys.*, vol. 45, no. 12, pp. 5461–5471, Dec. 2018.

[7] D. S. Kim and E. Lee, "Estimation of zero-frequency noise power density in digital imaging," *IEEE Signal Process. Lett.*, vol. 25, no. 11, pp. 1755–1759, Nov. 2018.

[8] X. Ji, M. Feng, R. Zhang, G. H. Chen, and K. Li, "A experimental method to correct drift-induced error in zero-frequency DQE measurement," in *Proc. SPIE, Med. Imag.: Phys. Med. Imag.*, vol. 10948, 2019, pp. 109 480H.1–109 480H.9.

[9] A. Gonzalez-Lopez and P.-A. Canpos-Morcillo, "Efficient detrending of uniform images for accurate determination of the noise power spectrum at low frequencies," *Phys. Med. Biol.*, vol. 64, no. 10, pp. 1–11, 2019.

[10] Y. Matsunaga, F. Hatori, H. Tango, and O. Yoshida, "Analysis of signal to noise ratio of photoconductive layered solid-state imaging device," *IEEE Trans. Electron Devices*, vol. 42, no. 1, pp. 38–42, Jan. 1995.

[11] J. H. Siewerdsen and D. A. Jaffray, "A ghost story: Spatio-temporal response characteristics of an indirect-detection flat-panel imager," *Med. Phys.*, vol. 26, no. 8, pp. 1624–1641, 1999.

[12] M. S. Bartlett, "Periodogram analysis and continuos spectra," *Biometrika*, vol. AE-37, nos. 1/2, pp. 1–16, Jun. 1950.

[13] P. D. Welch, "The use of fast Fourier transform for the estimation of power spectra: A method based on time averaging over short, modified periodograms," *IEEE Trans. Audio Electroacoust.*, vol. AE-15, no. 2, pp. 70–73, Jun. 1967.

[14] N. Mail, D. J. Moseley, J. H. Siewerdsen, and D. A. Jaffray, "An empirical method for lag correction in cone-beam CT," *Med. Phys.*, vol. 35, no. 11, pp. 5187–5196, 2008.

[15] J. Hsieh, O. E. Gurmen, and K. F. King, "Recursive correction algorithm for detector decay characteristics in CT," in *Proc. SPIE Med. Imag.: Phys. Med. Imag.*, vol. 3977, 2000, pp. 298–305.

[16] A. V. Oppenheim and R. W. Schafer, *Discrete-Time Signal Processing*, 3rd. ed. New York, NY, USA: Prentice-Hall, 2010.

[17] D. S. Kim, "Measurement of power density at zero frequency with a trend compensation," *IEEE Trans. Signal Process.*, vol. 68, pp. 1964–1973, 2020.

[18] D. S. Kim, "Noise power spectrum measurements in digital imaging with gain nonuniformilty correction," *IEEE Trans. Image Process.*, vol. 25, no. 8, pp. 3712–3722, Aug. 2016.

[19] M. B. Williams, P. A. Mangiafico, and P. U. Simoni, "Noise power spectra of images from digital mammography detectors," *Med. Phys.*, vol. 26, no. 7, pp. 1279–1293, Jul. 1999.

[20] Z. Zhou, F. Gao, H. Zhao, and L. Zhang, "Techniques to improve the accuracy of noise power spectrum measurements in digital X-ray imaging based on background trends removal," *Med. Phys.*, vol. 38, no. 3, pp. 1600–1610, Mar. 2011.

[21] P. Billingsley, *Probability and Measurement*. Hoboken, NJ, USA: Wiley, 1995.

[22] J. Starman, J. Star-Lack, G. Virshup, E. Shapiro, and R. Fahrig, "A nonlinear lag correction algorithm for a-Si flat-panel X-ray detectors," *Med. Phys.*, vol. 39, no. 10, pp. 6035–6047, 2012.

[23] S. Freestone, R. Weisfield, C. Tognina, I. Job, and R. E. Colbeth, "Analysis of a new indium gallium zinc oxide (IGZO) detector," in *Med. Imag. 2020: Phys. Med. Imag.*, G.-H. Chen and H. Bosmans, Eds., vol. 11312. Bellingham, WA, USA: International Society for Optics and Photonics, 2020, pp. 970–976.